

Boise State University
ScholarWorks

Materials Science and Engineering Faculty
Publications and Presentations

Department of Materials Science and Engineering

3-1-2014

Identification of Silver and Palladium in Irradiated TRISO Coated Particles of the AGR-1 Experiment

I. J. van Rooyen
Idaho National Laboratory

T. M. Lillo
Idaho National Laboratory

Y. Q. Wu
Boise State University

NOTICE: this is the author's version of a work that was accepted for publication in *Journal of Nuclear Materials*. Changes resulting from the publishing process, such as peer review, editing, corrections, structural formatting, and other quality control mechanisms may not be reflected in this document. Changes may have been made to this work since it was submitted for publication. A definitive version was subsequently published in *Journal of Nuclear Materials*, (2014). DOI: 10.1016/j.jnucmat.2013.11.028

Identification of Silver and Palladium in Irradiated TRISO Coated Particles of the AGR-1 Experiment

I. J. van Rooyen

Fuel Performance and Design Department
Idaho National Laboratory
Idaho Falls, ID 83415-6188, USA

* Corresponding author. Tel +1208 526 4199

E-mail address: Isabella.vanRooyen@inl.gov

Y.Q. Wu

Department of Materials Science and
Engineering

Boise State University
Boise, ID 83725-2090, USA

and

Center for Advanced Energy Studies
Idaho Falls, ID 83401, USA

T. M. Lillo

Materials Science & Engineering Department
Idaho National Laboratory
Idaho Falls, ID 83415-6188, USA

Abstract

Evidence of the release of certain metallic fission products through intact tristructural isotropic (TRISO) particles has been seen for decades around the world, as well as in the recent AGR-1 experiment at the Idaho National Laboratory (INL). However, understanding the basic mechanism of transport is still lacking. This understanding is important because the TRISO coating is part of the high temperature gas-cooled reactor functional containment and critical for the safety strategy for licensing purposes.

Our approach to identify fission products in irradiated AGR-1 TRISO fuel using scanning transmission electron microscopy (STEM), Electron Energy-Loss Spectroscopy (EELS) and Energy Filtered TEM (EFTEM), has led to first-of-a-kind data at the nano-scale indicating the presence of silver at triple-points and grain boundaries of the SiC layer in the TRISO particle. Cadmium was also found in the triple junctions. In this initial study, the silver was only identified in SiC grain boundaries and triple points on the edge of the SiC-IPyC interface up to a depth of approximately 0.5 μm .

Palladium was identified as the main constituent of micron-sized precipitates present at the SiC grain boundaries. Additionally spherical nano-sized palladium rich precipitates were found inside the SiC grains. No silver was found in the center of the micron-sized fission product precipitates using these techniques, although silver was found on the outer edge of one of the Pd-U-Si containing precipitates which was facing the IPyC layer. Only Pd-U containing precipitates were identified in the IPyC layer and no silver was identified in the IPyC layer.

The identification of silver alongside the SiC grain boundaries and the findings of Pd inside the SiC grains and alongside SiC grain boundaries provide important information needed to understand silver and palladium transport in TRISO fuel, which has been the topic of international research for the past forty years. The findings reported in this paper may support the postulations of recent research that Ag transport may be driven by grain boundary diffusion. However, more work is needed to fully understand the transport mechanisms. Additionally, the usefulness of the advanced electron microscopic techniques for TRISO coated particle research is demonstrated in this paper.

Keywords: 3C-SiC, TRISO, STEM, EELS, EFTEM, Ag transport mechanism

1. Introduction

Evidence of the release of certain metallic fission products e.g. Ag and Pd, through intact tristructural isotropic (TRISO) particles has been seen for decades around the world, as well as in the recent AGR-1 experiment at Idaho National Laboratory (INL) [1; 2]. The TRISO coating is part of the high temperature gas-cooled reactor functional containment and critical for the safety strategy for licensing purposes. This enhances the importance of identifying the metallic fission product release (transport) mechanisms through these containment layers. Specifically understanding the transport mechanism of ^{110m}Ag is of importance as the release of ^{110m}Ag is a potential worker safety concern due to plate-out on the cooler metallic parts of the helium pressure boundary. This plate-out of ^{110m}Ag can pose a potential risk for maintenance personnel. Although silver releases were measured outside the TRISO coated particles during post irradiation examination (PIE) during the German AVR program, and later similar programs including the recent AGR-1 experiment at INL [1; 2;], no silver was identified in the SiC layer, which is the main barrier for fission products, of irradiated fuel.

Numerous mechanisms for such Ag transport during neutron irradiation were derived from reactor experimentation release data, out-of-pile experimentation under simulated conditions and empirical studies over the past 38 years [3; 4]. Furthermore, individual studies and results have supported a variety of possible ^{110m}Ag transport mechanisms that may also occur in TRISO fuel under neutron irradiation. Grain boundary diffusion has been suggested and discussed as a possible transport mechanism in neutron irradiated TRISO coated particles as early as 1975 by Nabielek et al., [5]. More recent out-of-pile experimental on SiC and computational work also indicated that Ag transports via grain boundary diffusion under their specific experimental conditions [6–10]. Experimental evidence by Lopez-Honorato, et al., [8] using scanning electron microscopy; indicated that silver accumulated at grain boundaries in unirradiated SiC layers of a simulated TRISO coated particle experiment. They concluded that silver diffusion was strongly affected by grain boundary diffusion. Although consideration was given in their studies to bulk movement and that nucleation of Ag occurred at grain boundaries only during cooling, bulk diffusion was ruled out based on theoretical work by Chen et al., [11]. This work did not support the hypothesis of silver transport through nano cracks as previously suggested by MacClean [12]. Furthermore, bulk diffusion has also been shown computationally to be many orders of magnitude smaller than grain boundary diffusion [9; 10]. These results on unirradiated SiC are insightful but suffer from important differences relative to irradiated TRISO particles: (a) the concentration of Ag used in the experiments is much greater than that expected in an actual TRISO particle, (b) unirradiated specimens, or ion versus neutron irradiation are used in many cases, and (c) differences in fabrication process condition of the SiC used for experimental out-of-pile studies. For example, at the low concentrations of Ag anticipated in a TRISO particle, others have argued that the mechanism of vapor transport may be more applicable [3; 12].

In order to evaluate the applicability and significance of these out-of-pile transport mechanisms, as well as transport mechanisms unique to neutron irradiation such as enhanced bulk diffusion due to neutron irradiation-induced defects, the full characterization of microstructural and composition information, and specifically the identification of Ag in the SiC layer of actual irradiated TRISO coated particles, needs to be obtained for irradiated TRISO fuel. Thus, there is a need to examine the behavior of Ag in irradiated TRISO particles to help improve our understanding of the transport behavior of Ag in TRISO particles.

The initial electron microscopic examination on the INL AGR-1 coated particles using scanning electron microscopy (SEM), energy dispersive spectroscopy (EDS), wavelength dispersive spectroscopy (WDS), and transmission electron microscopy (TEM) attempted to identify silver in fission-product precipitates. Although evidence of fission product precipitates were found in the SiC on SiC grain boundaries and IPyC layers, no silver was conclusively identified [13]. It was speculated that Ag would be able to substitute for Pd in a $\text{U}(\text{Ag},\text{Pd})_2\text{Si}_2$ solid solution rather than forming a separate phase since they have identical atomic radii (both 0.144 nm for the pure elements [14]). Additionally, nano-sized voids aligned at the grain boundaries have been found in the vicinity of a fission product precipitate [14]. Investigations are in progress to determine a possible link to fission product transport. This, therefore, highlighted the important need for identifying silver in the irradiated SiC layer of a TRISO coated particle and to provide more detailed quantification and identification of the fission product precipitates found during the initial examination.

Palladium is also a metallic fission product of great interest in TRISO fuel. Past studies have shown that Pd can corrode SiC [15-17] and it has been postulated to be a potential failure mechanism at high burnup in low-enriched TRISO fuels when temperatures exceed 1100°C. Characterization studies by Barrachin et al., [15] on HFR-EU1bis experiments on UO₂ TRISO fuel (10.2% FIMA, calculated pebble centre temperature of 1250°C) found that Pd is specifically present in the inner pyrocarbon layer at the inside of the SiC layer, but no Pd is mentioned in the SiC layer itself. Neethling et al. [18] showed that Ag transport in SiC took place when present at the SiC surface as a Ag-Pd mixture. No penetration of the SiC layer was found in the absence of Pd. Results of this study (and others [17]) indicate Pd reacts with Si to form Pd₂Si and graphite regions form due to the carbon remaining (re-precipitated) after the formation of the silicides. These studies further showed significant Pd corrosion on the SiC-PyC interface. However, in the AGR-1 experiment, no significant Pd corrosion is observed [13]. The Pd and Ag concentrations used in these out-of-pile research studies, are order of magnitude larger than in the actual TRISO coated particles, which could contribute to the different corrosion behaviour observed compared to those of the AGR-1 experiment. Our understanding of its behavior in UCO TRISO fuel is also incomplete and is therefore further explored in this study.

This paper reports the results utilizing scanning transmission electron microscopy (STEM), STEM-EDS, electron energy loss spectroscopy (EELS) and energy filtered transmission electron microscopy (EFTEM) obtained from a selected irradiated TRISO fuel particle. These STEM, EELS and EFTEM investigations are first-of-a-kind for irradiated TRISO coated particles and more details on the choice of these techniques, are provided in section 2.2. Since the main focus of this publication is the identification and quantification of the elemental composition of fission products; specifically the identification of Ag in irradiated SiC, the grain boundary characteristics of the SiC layer of the irradiated baseline fuel are not included and will be discussed in a separate publication. However, this work provides new evidence at both the micrometer and nanometer scale that will help improve the understanding of Ag and Pd transport behavior in irradiated TRISO fuel. This paper also provides the first direct evidence of Ag in a neutron irradiated SiC layer of TRISO coated particles under VHTR reactor conditions.

2. Material and methods

2.1 Material

Because of the importance of silver behavior in TRISO fuel, specific particles were chosen for analysis as part of this study based on the degree of silver retention exhibited during irradiation. Individual particles from selected deconsolidated compacts were gamma counted to measure the activity of various gamma-emitting fission products [2]. The initial results of the advanced electron microscopic examination of selected coated particles from Compact 6-3-2 from Capsule 6 are presented in this paper. Compact 6-3-2 contains baseline fuel fabricated with coating process conditions similar to those used to fabricate historic German fuel because of its excellent irradiation performance with UO₂ kernels. The AGR-1 fuel is, however, made of low-enriched UCO (uranium oxycarbide). Kernel diameters are approximately 350 μm with a U-235 enrichment of approximately 19.7%. Selected properties for the baseline AGR-1 coated particles are shown in Table 1 [19].

Table 1. Selected properties (Mean Value ± Population Standard Deviation) for the AGR-1 baseline coated particles [19]

| Property | Mean value ± Population standard deviation | |
|----------|--|------------------------------|
| | Thickness (μm) | Density (mg/m ³) |
| Buffer | 103.5 ± 8.2 | 1.10 ± 0.04 |
| IPyC | 39.4 ± 2.3 | 1.904 ± 0.014 |
| SiC | 35.3 ± 1.3 | 3.208 ± 0.003 |
| OPyC | 41.0 ± 2.1 | 1.907 ± 0.008 |

Compact 6-3-2 was irradiated to a 11.3% FIMA average burnup, 1070°C time-average, volume – average temperature; 1144°C time-average, peak temperature and an average fast fluence of 2.38×10^{21} n/cm².

The retention of ^{110m}Ag in each particle is estimated by comparing the measured inventory to the predicted inventory normalized by the relative Cs-137 activity to reduce the influence of different kernel sizes on the overall distribution (please see [2] for detail). The measured-to-calculated ratio for 60 gamma counted particles from Compact 6-3-2 ranged from 0.075 to 0.882. Coated particle AGR1-632-035 was selected because it exhibited a higher than average retention of ^{110m}Ag under irradiation compared to other particles from the same compact, in the hope that enough Ag would be present to be identified using these advanced microscopic characterization techniques. The measured-to-calculated ^{110m}Ag ratio for particle AGR1-632-035 was 0.787.

2.2 Methods

The coating layers on the high temperature gas-cooled reactor fuel consist of relatively light elements such as carbon and silicon. The fission products produced during irradiation consists of relatively heavy elements which migrated into these coatings. High Angle Annular Dark Field (HAADF) detector is best suited for characterization studies, easily differentiating between the pyrolytic graphite and SiC coatings as well as revealing the distribution of fission products. The HAADF detector in the scanning transmission electron microscopy (STEM) mode discriminates only differences in atomic number (so-called Z-contrast imaging). This mode is most useful in the identification of small precipitates for further compositional analysis [-20]. Additionally, compositional analysis of small precipitates and second phases using transmission electron microscopy (TEM) with energy dispersive spectroscopy (EDS) requires two main characteristics – namely, a small electron probe (smaller than the feature under analysis) and the collection of an EDS spectrum suitable for quantification of the elements present. Technological advances in state-of-the-art TEMs have made it possible to form extremely small probe sizes. Particularly in the STEM mode, probe sizes around 1 nm or less are possible. In STEM imaging mode, a small electron probe is scanned across the sample and an image of the sample is built up pixel-by-pixel from information collected by the HAADF detector below the sample. Generally, the time to collect an EDS spectrum with a high signal-to-noise ratio increases as the electron probe size decreases. However, when a high brightness, Field Emission Gun (FEG) electron source is used, the EDS spectrum collection time becomes reasonable. The STEM used for the work reported in this paper was conducted with a microscope with a FEG electron source.

In our strategy to identify silver, another analytical tool namely electron energy loss spectroscopy (EELS) is considered. In TEM, some incoming electrons lose energy when they travel through the specimen due to the inelastic interaction with specimen's atoms. EELS analyzes the energy distribution of these scattered electrons and provides quantitative compositional information about the nature of the atoms under illumination by the electron beam. The transmitted electrons can be filtered with respect to energy loss and only those electrons with a specific energy loss, e.g., that associated with Ag can be chosen for imaging. In essence, these filtered electrons, with a selected energy loss, form an elemental map in the imaging mode (EFTEM). EELS analysis is considered important for TRISO fuel research because of the specific resolution of elements of interest. In EELS analysis, the chemical sensitivity and the size of resolvable feature could be at 1% and smaller than 1 nm, respectively. Moreover, Pd, Ag and U have close but separable edge energies in an EELS spectrum, which suggests that trace amounts of Ag in the studied sample should be able to be detected using the EELS technique. EELS/EFTEM requires thin TEM specimens.

The STEM and EELS analyses were conducted with a FEI Tecnai G2 F30 STEM at the Microscopy and Characterization Suite (MaCS), Center for Advanced Energy Studies (CAES) at INL, where low activity irradiated materials can be examined. The thin, focused ion beam (FIB)-prepared lamellas minimized irradiation dose to a level that enable us to use these advanced techniques for the irradiated TRISO coated particles. The specimen was prepared at the Electron Microscopy Laboratory (EML) at the Materials and Fuels Complex (MFC) of INL using the dual-beam Quanta 3D FEG FIB (Figure 1). For this paper, the results obtained from examining the FIB lamella at position 6b are discussed. This lamella was extracted from a location approximately tangent to the SiC-IPyC interface and contains parts of both the IPyC- and SiC layers as shown in Figure 1c.

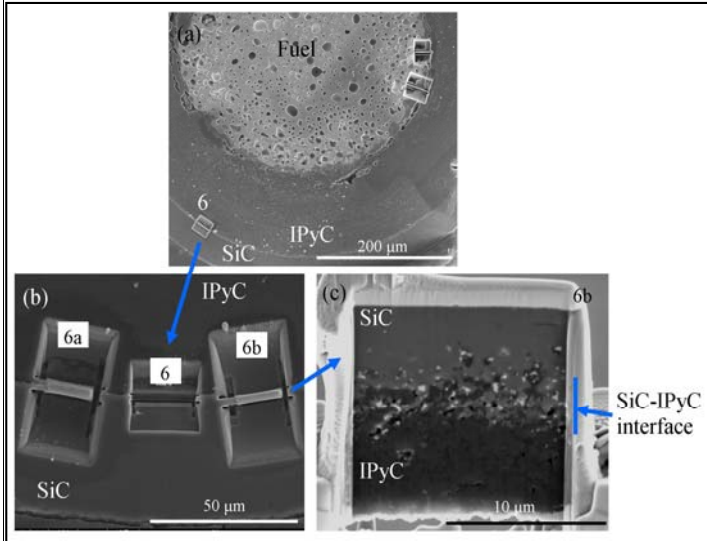


Figure 1: Images showing the (a) the cross sectioned mounted coated particle AGR1-632-035, (b) the FIB lamella position 6b and (c) the AGR1-632-035-6b FIB lamella consisting of the SiC-IPyC interface at higher magnification.

2.3 Approach followed for the STEM examination

Three areas were identified for the initial STEM examination: the SiC-IPyC interlayer, a region deeper inside the SiC layer and another region in the IPyC layer further away from the SiC-IPyC interface. During these examinations, attention was given to the precipitates on the outer edge of the SiC-IPyC interface because this is the starting point for the transport of fission products as they move from the IPyC to the SiC. Color-coded numbers shown in Figure 2 are used to indicate the five areas examined at the SiC-IPyC interface (yellow numbers 1 to 5), the one area further in the SiC layer (red number 6) and the one area in the IPyC (green number 7). The investigation focused on identifying the elemental components in the precipitates using EDS line and spot scans, and on determining the physical nature of the precipitates (i.e., inter- or intragranular).

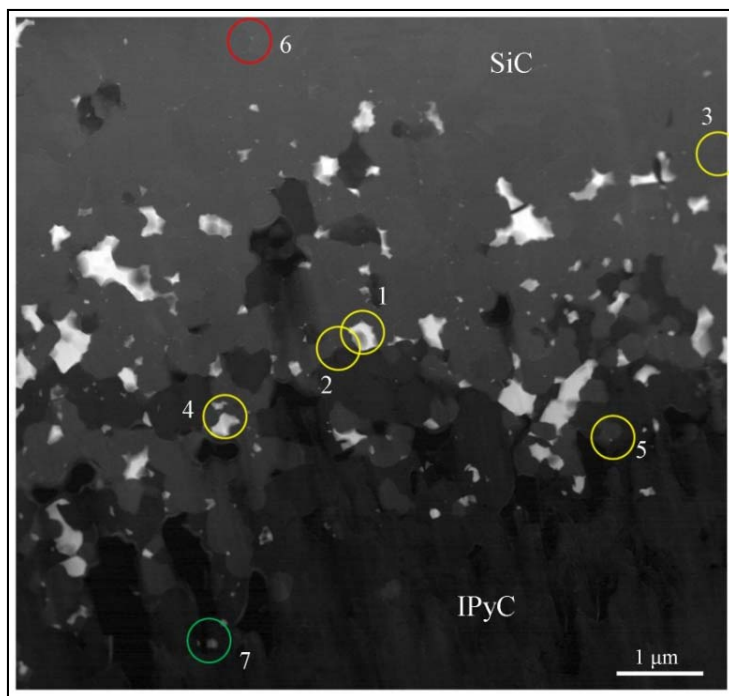


Figure 2: STEM Z-contrast micrograph using the high-angle annular dark-field (HAADF) detector showing the three main examination areas: the SiC-IPyC interlayer (yellow numbers 1 to 5), deeper inside the SiC layer (red number 6) and the IPyC layer further away from the SiC-IPyC interlayer (green number 7).

3. Results and Discussion

3.1 Identification of Silver using STEM-EDS

Silver was identified in specific locations in areas 1 through 4 using the STEM-EDS detector by focusing at the higher energies associated with K level transitions of the fission products. The higher energies allowed us to identify silver in the presence of high levels of palladium, without the interference and overlap problems associated with lower energy x-ray peaks. The palladium and silver $K\alpha_1$ peaks are separated by approximately 1 keV (21.175 keV vs. 22.162 keV, respectively). (The uranium $L\gamma_1$ peak is located at 20.163 keV and also does not overlap the peaks of the fission products). Figure 3 shows the presence of silver along the grain boundary leading up to a micron-sized precipitate in area 1. No silver was found in the micron-sized precipitate in area 1 which was predominantly found to contain Pd, U and Si. The EDS line scan is normalized to the three elements Pd, U and Ag only.

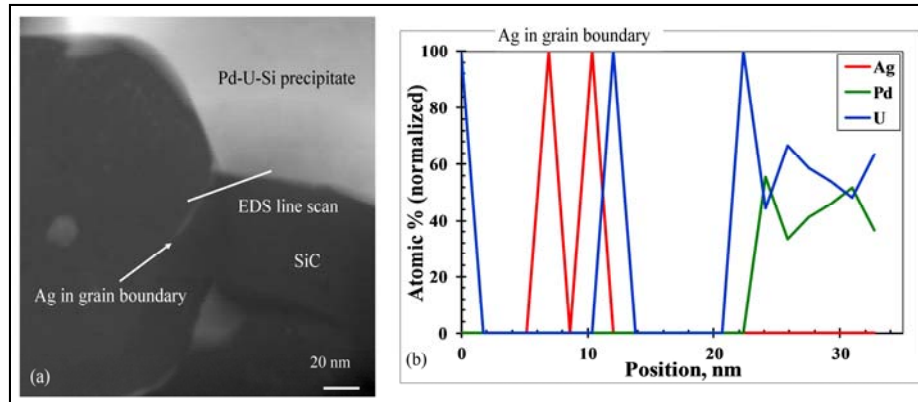


Figure 3: Images showing the (a) the HAADF STEM image of a silver-containing grain boundary and (b) the EDS line scan confirming the presence of silver in the grain boundary leading up to the micron-sized Pd-U-Si precipitate.

More significantly, silver was identified in both the grain boundaries (marked 1 and 2 in Figure 4) leading up to the triple junction (marked 3 in Figure 4) and in the triple junction itself in the SiC layer near the edge of the IPyC. The EDS spectrum from the center of this triple junction shown in Figure 5a identifies the Ag K peak at 22.162 keV. It is also interesting to note that Cd, at 23.172 keV in Fig. 5a, is observed in this triple junction. (Cd is a metallic fission product as well.) No Pd is however observed in this triple junction although Pd is identified in the SiC matrix adjacent to this triple junction as shown in Figure 5b and Figure 5c from the EDS line scan through this triple junction (marked 3 in Figure 4) as well as in the higher magnification of this area shown respectively.

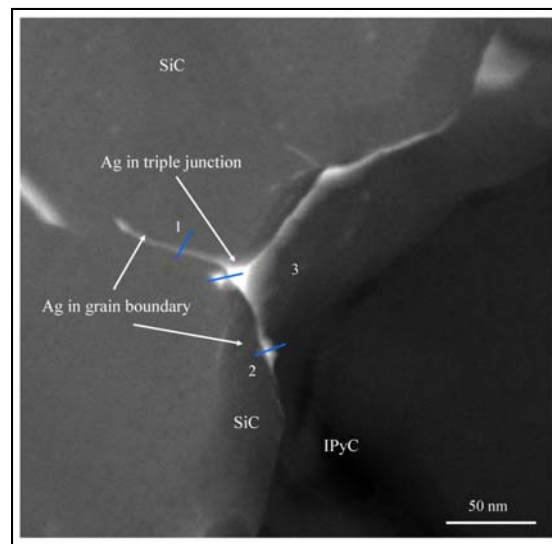


Figure 4: Image showing the HAADF STEM image of silver-containing grain boundaries and triple junction at the outmost edge of the SiC adjacent to the IPyC at area 2 shown in Figure 2.

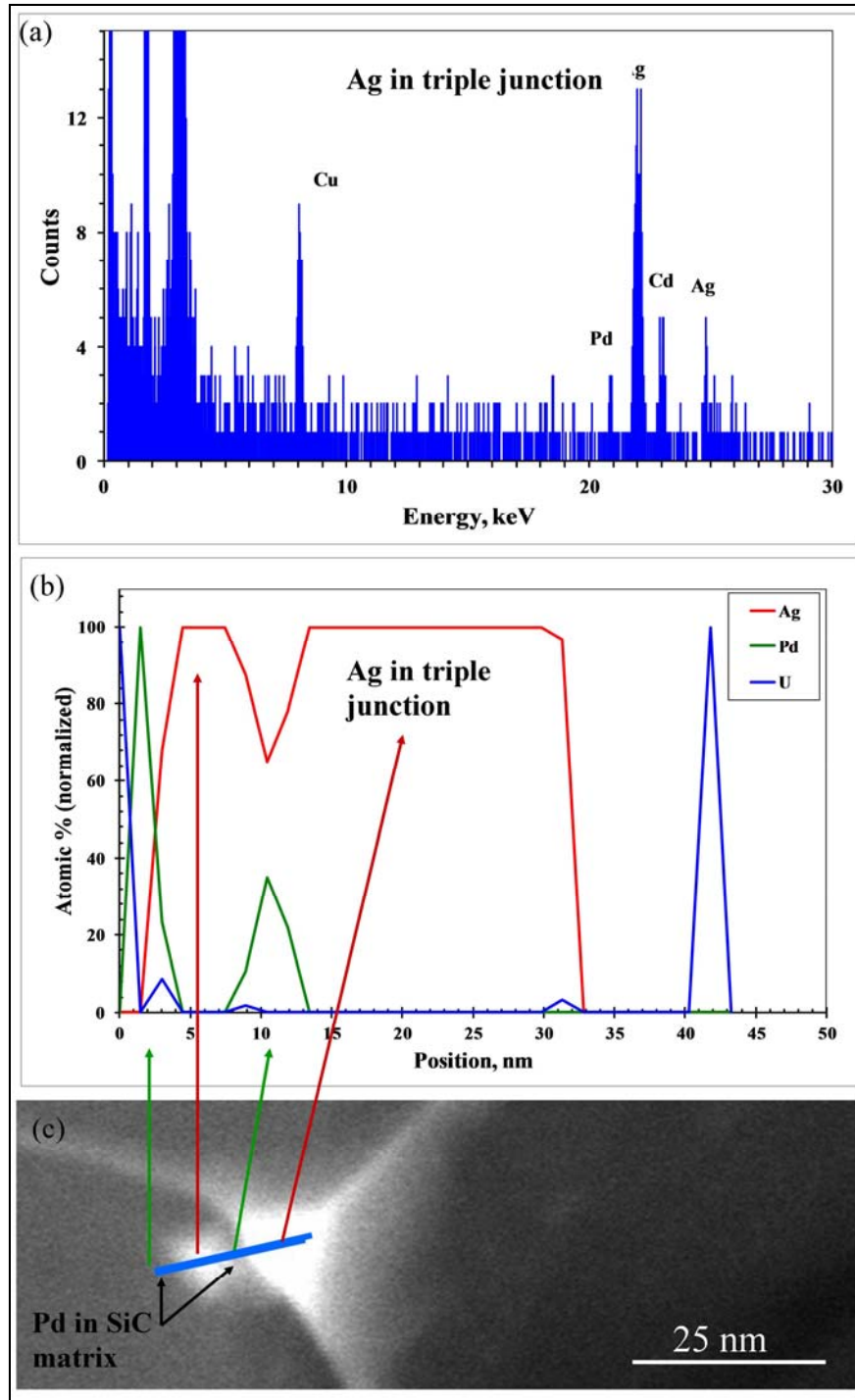


Figure 5: Image showing (a) the EDS spectrum identifying the Ag K peak at 22.162 keV and the presence of Cd in the centre of the triple junction shown in Figure 4, (b) the EDS line scan profile through the triple junction indicating the presence of Ag (Cu is an artifact from the grid holder), and (c) higher magnification of the area 3 in Figure 4, showing the presence of Pd in the SiC matrix adjacent to this triple junction

Area 3 of Figure 2 was also found to contain grain boundaries with significant concentrations of silver. This area contained a high density of triple junctions in somewhat of a curious configuration, Figure 6. An EDS line scan was performed along the blue line at the triple junction in Figure 6. The EDS spectra from the point in the line scan with the highest silver content is shown, Figure 7a, while the complete composition profile across the triple junction is shown in Figure 7b. It is evident that silver is present throughout this particular triple junction. However, this was not necessarily the case for all triple junctions in this area. In fact, only four showed significant silver content while three showed no evidence of silver and two others exhibited only possible indications of silver from extremely small Ag EDS peaks, probably due to very low concentrations of Ag. Additionally, Ag-free (or low Ag concentration) triple junctions appear to be connected to Ag-rich triple junctions via grain boundaries and, thus, suggest that grain boundary character may have an influence on silver transport. Transmission Electron Back-Scattered Diffraction (t-EBSD) analysis of the grain and grain boundary orientation relationships is being planned for this and other samples in an effort to understand the effect of grain boundary parameters on fission product transport.

However, the fact that not all the triple junctions contain silver, leads to questions regarding the role of grain boundary type on silver transport and collection at triple points. Does this mean for example that triple junctions rich in silver consist of one grain boundary capable of easily transporting silver to the triple junction and two grain boundaries incapable of transporting silver efficiently away from the triple junction, thus resulting in a silver-rich triple junction? Or is it that the Ag-free triple junction does not contain a grain boundary that is capable of transporting silver to the junction while the low-Ag triple junctions may have grain boundaries that transport the silver away from the triple junction at a slightly slower rate than the grain boundary supplying the silver to it? Future research work is needed to answer these questions. If these questions can be answered and future work shows that grain boundaries with varying silver transport capabilities do exist, the silver distribution in Figure 6 could be explained. Additional work to characterize the boundaries is required to further understand the potential role that grain boundary character plays in silver transport.

A fine network of the Pd/Ag containing material is visible on grain boundaries up to approximately 4 μm inside the SiC layer, although this needs to be explored further for maximum depth visibility. It was for example found in the earlier studies [7] that the micron-sized Pd-rich precipitates were visible up to approximately 15 μm into the SiC-layer.

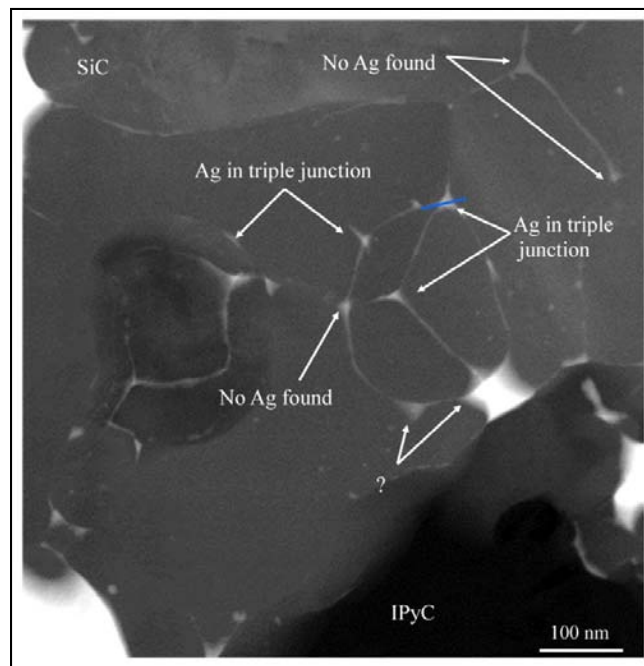


Figure 6: Photomicrograph of area 3 showing the triple junctions analyzed. Junctions found to contain or not contain Ag are indicated while those where the EDS results for Ag were ambiguous are marked with “?”.

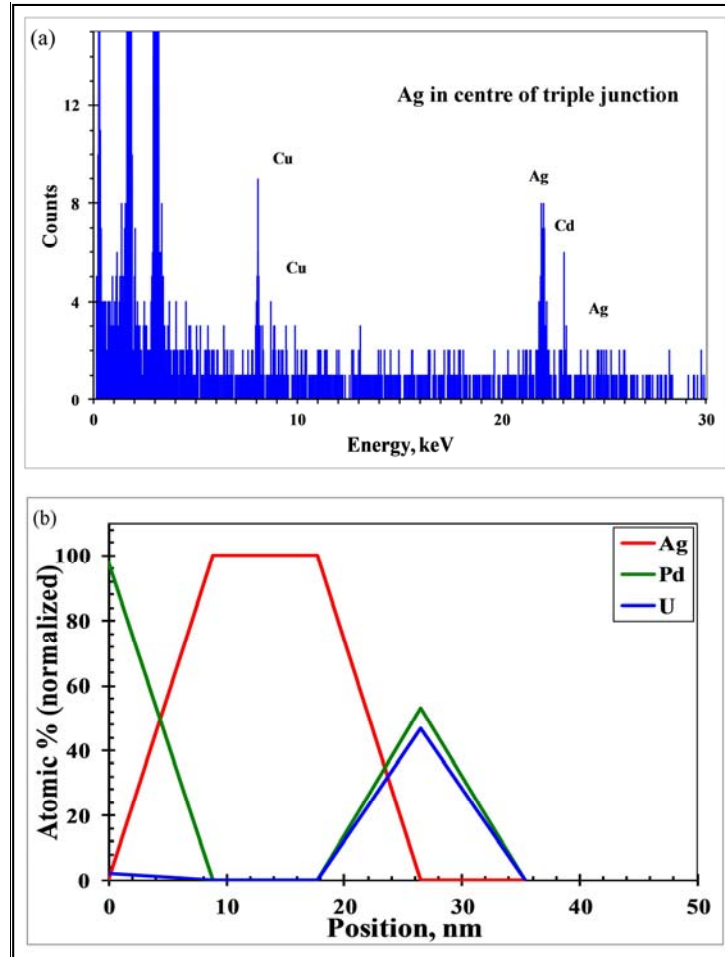


Figure 7: a) EDS spectra from the center of the triple junction in Figure 6 at the blue line showing the presence of silver and b) the composition profile across the triple junction, normalized to elements U, Ag and Pd only.

Silver was also found in conjunction with coarse palladium precipitates. Figure 8 shows a palladium- and uranium-containing precipitate, as indicated by the EDS spectra, Figure 8b, taken from the center of the bright precipitate. The concentration profile in Figure 8c, was obtained from EDS line scan data along the white line shown in Figure 8a, spanning the IPyC/precipitate interface, and, again, normalized to three elements of interest. A small amount of Ag is found only at the interface between the IPyC and the Pd, U-containing precipitate.

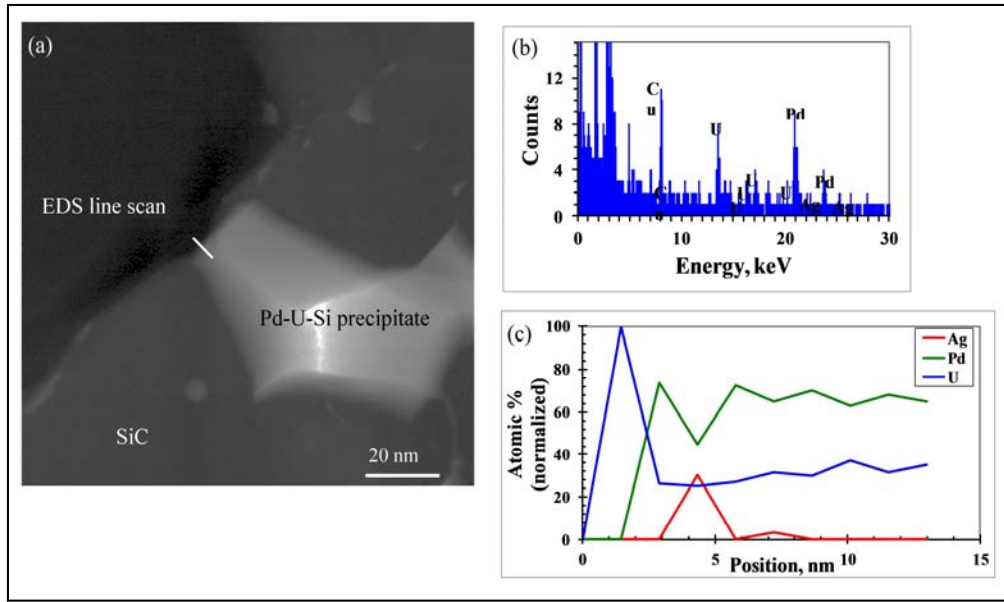


Figure 8: (a) Pd,U – containing precipitate on the IPyC/SiC interface showing the location of the EDS line scan in (c) and (b) the EDS spectrum from the interior of the precipitate showing significant levels of Pd and U with virtually no Ag present. c) The composition profile acquired along the white line in (a), shows silver present at the IPyC/precipitate interface only.

3.2 Identification of Silver using EELS and EFTEM

Ag, Pd and U can also be distinguished by using EELS since their edge energies are separated from each other (i.e., Pd M_{4,5} 335 eV, Ag M_{4,5} 367 eV, U N₇ 381 eV)[21]. Therefore, EELS was carried out at area 2 (Figures 2 and 4) where an Ag-rich intergranular phase was found by EDS (Figure 5) to verify the presence of silver and further investigate the Ag behavior.

Figure 9a is a zero-loss image of the triple-junction area and the triple junction phase is in darker contrast in this image. A corresponding EELS spectrum in a range from ~ 230 eV to ~ 390 eV within this area is shown in Figure 9b. It can clearly be seen from this spectrum that the Ag M_{4,5} peak (367 eV) is detected, direct evidence of a Ag-rich phase along the grain boundaries. A very small peak at 340 eV is also observed in the spectrum, which likely corresponds to a Pd M_{4,5} peak, indicating this area may also contains some amount of Pd, although this needs validation. EFTEM elemental maps of Ag and Si were also obtained at this triple-junction area, as shown in Figures 9c and 9d, respectively. In the EFTEM elemental map, the lighter region corresponds to the elements being analyzed. Therefore, Figure 9c clearly shows the triple-junction phase is Ag-rich; and Figure 9d indicates this triple-junction area is located at the boundary between SiC and IPyC phases.

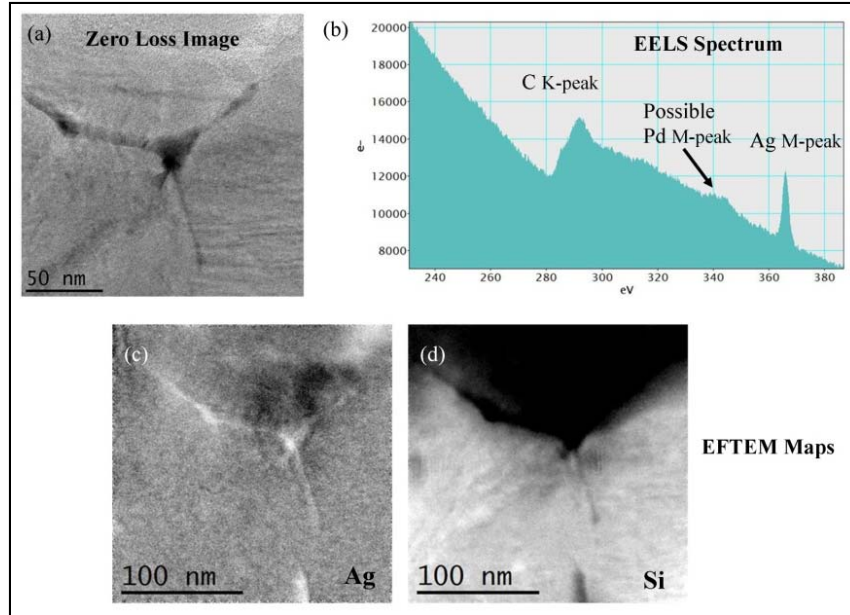


Figure 9 Zero-loss image of the second phase at triple junction (a) and corresponding EELS spectrum obtained at this area (b); EFTEM elemental maps of Ag and Si at this area (c) and (d), respectively.

3.3 Identification of Palladium

EDS analyses were also carried out on and in the vicinity of a large precipitate (area 1 in Figure 2) about one-half micron away from the triple-junction area where the Ag-rich phase was detected (Figures 4 and 9). Figure 10a is a STEM High Angle Annular Dark Field (HAADF) image of this precipitate. EDS area scans (~ 200 nm \times 150 nm and ~ 50 nm \times 10 nm) both inside and at the edge of this precipitate reveal that this is a Pd-U-Si phase (Figure 10b). Interestingly, sphere-shaped precipitates of $\sim 10 - 20$ nm size are observed inside the SiC grains near the SiC-IPyC phase boundaries (Figure 11 a), as well as approximately 4 μ m inside the SiC layer (Figure 11b; area 6 in Figure 2). These precipitates have a lighter contrast than the SiC matrix in the STEM HAADF images shown in Figures 11a and b. EDS analyses (Figure 11c and d) reveal that these nano-precipitates are Pd-rich phases. Further work is needed to identify the complete composition and crystal structure of these precipitates.

During STEM observation, irregular shaped precipitates in light contrast and about less than 100 nm size were found inside the IPyC layer (Figure 12). EDS analyses were carried out on these precipitates and the results indicated that they are Pd-U rich phases. No silver was identified in the precipitates examined in the IPyC layer.

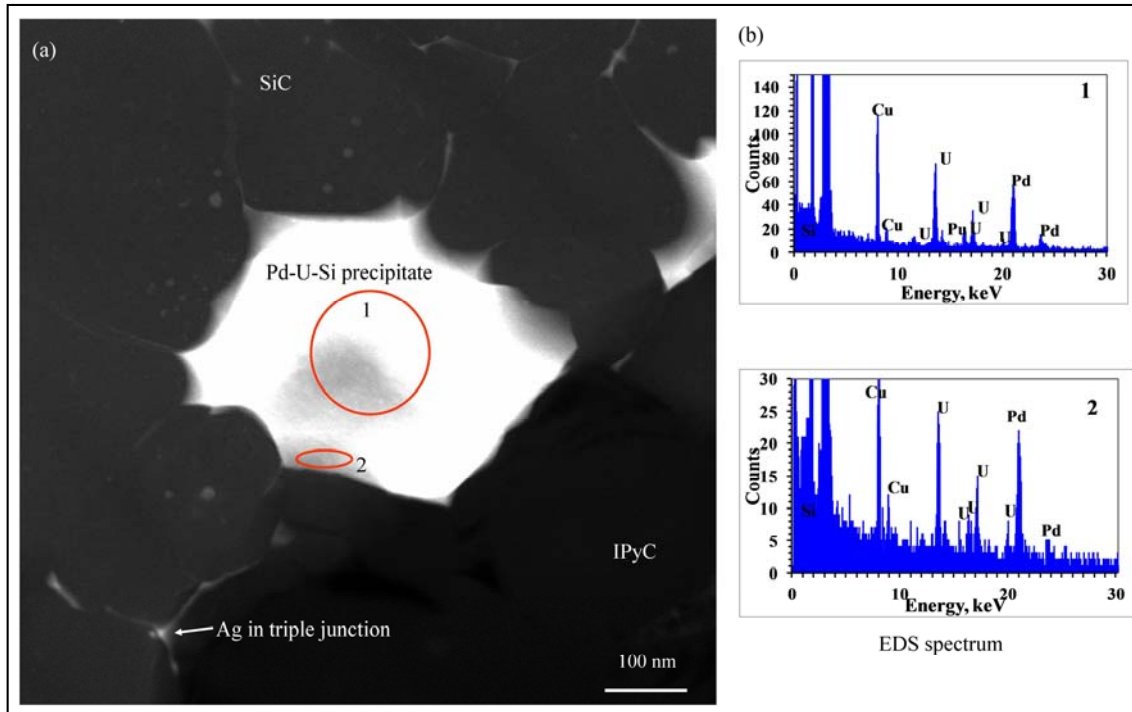


Figure 10: A STEM High Angle Annular Dark Field (HAADF) image of a large precipitate shown in (a) with the EDS area scans ($\sim 200 \text{ nm} \times 150 \text{ nm}$ and $\sim 50 \text{ nm} \times 10 \text{ nm}$) both inside and at the edge of this precipitate reveal that this is a Pd-U-Si phase (Figure 10b). Ag is detected at the grain boundary extended from this precipitate (Cu is an artifact from the grid holder).

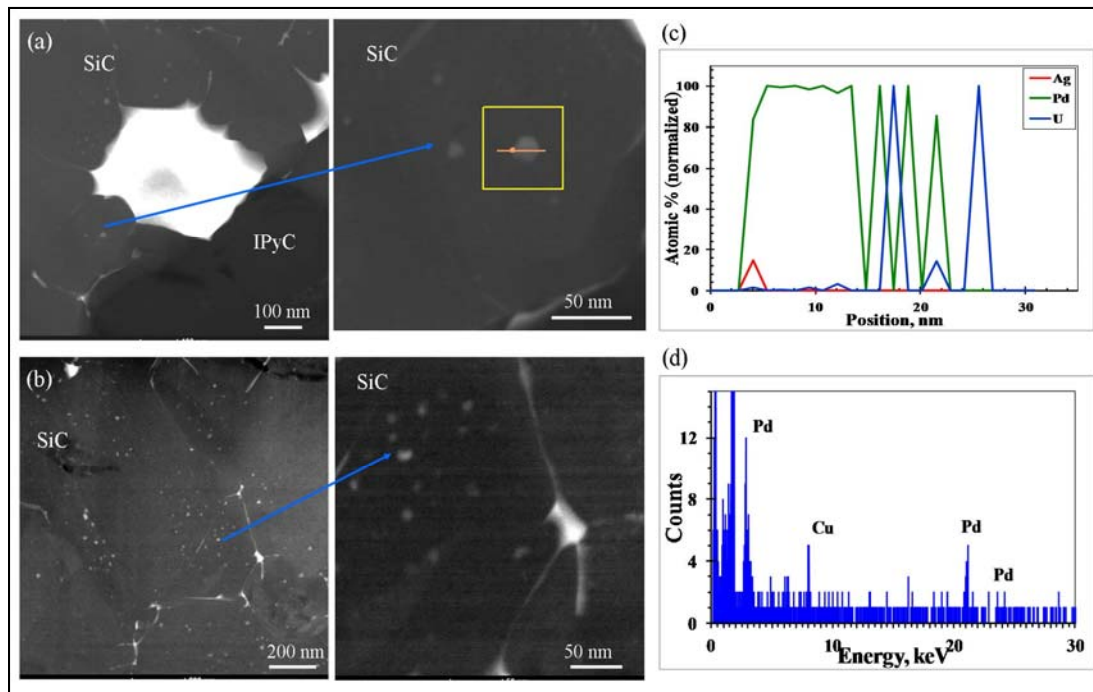


Figure 11: STEM HAADF images showing nanometer-size precipitates ($\sim 10 - 20 \text{ nm}$) inside SiC grains (a) at the SiC-IPyC interface and (b) approximately $4 \mu\text{m}$ inside the SiC layer. The corresponding EDS line scan and spectrum respectively in (c) and (d) revealed that these are a Pd-containing phase.

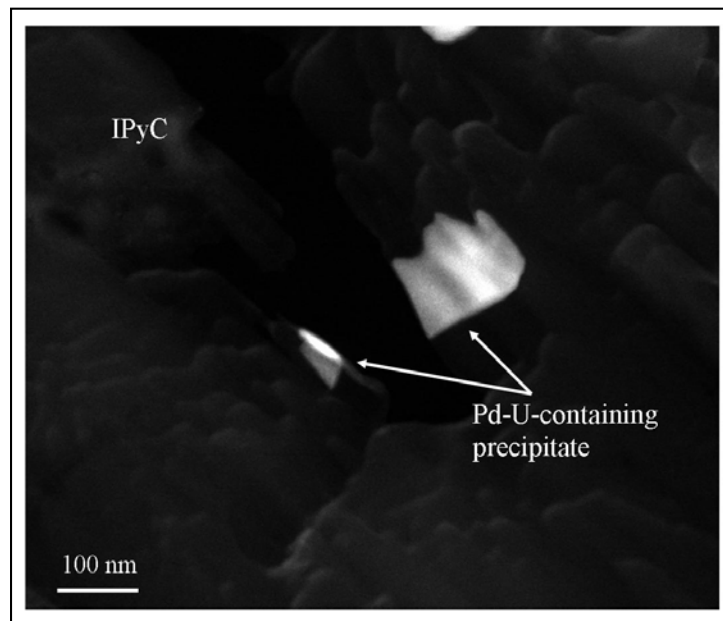


Figure 12: STEM HAADF images showing Pd-U rich irregular shaped precipitates of about 100 nm size in light contrast inside the IPyC layer. No silver was identified in the precipitates examined in the IPyC layer.

4. Conclusions

STEM, EELS and EFTEM were used to identify for the first time the physical location and elemental distribution of fission products at the micro- and nano-scale in the SiC and IPyC layers of irradiated TRISO fuel. Additionally, the STEM examination provided evidence of nano-sized silver precipitates at triple-points and grain boundaries in the SiC on the edge of the SiC-IPyC interface up to a depth of approximately 0.5 μm . Cadmium was also found to be present in the triple junctions.

Palladium was identified as the main constituent of the micron-sized precipitates present at the SiC grain boundaries which confirmed the preliminary studies by Van Rooyen et al., [-13]. Additionally spherical nano-sized palladium-rich precipitates were found inside the SiC grains. These nano-sized Pd precipitates were found to be distributed up to a depth of approximately 4 μm away from the SiC-IPyC interlayer. No silver was found in the center of the micron-sized fission product precipitates using these techniques, although silver was found on the outer edge of one of the Pd-U-Si containing precipitates which was facing the IPyC layer. Only Pd-U containing precipitates were identified in the IPyC layer and no silver was identified in the IPyC layer.

A fine network of the Pd/Ag containing material is visible on grain boundaries up to approximately 4 μm inside the SiC layer, although this needs to be explored further. It was for example found in the earlier studies [13] that the micron-sized Pd-rich precipitates were visible up to approximately 15 μm from the SiC/IPyC interface.

The identification of silver alongside the grain boundaries and the findings of Pd inside the grains and alongside grain boundaries provide significant knowledge to better understand silver and palladium transport behavior in TRISO fuel, which has been a topic of international research for the past forty years. Understanding the mechanism is important because the TRISO coating is part of the HTGR functional containment.

As silver was identified in the SiC grain boundary structure, investigations following the silver-containing grain boundary networks can lead to more clarity on the silver transport mechanism through the SiC structure. For example, grain and grain boundary character determination between triple points where silver was found can provide information on preferred orientations for silver transport pathways. Additionally, EFTEM maps and detailed EELS analysis on larger (micron-sized) precipitates will provide more compositional detail; while the atom probe analysis will provide 3D elemental maps which will provide information on transport mechanisms.

The transmission electron back scattered diffraction (t-EBSD) technique is being considered for TRISO coated particle research in parallel to EBSD studies on irradiated SiC. This technique may provide advantages not only in decreased sample preparation time, but also in the quality and resolution of results needed when studying fission product transport in irradiated SiC. This will also provide a direct means to measure the grain characteristics at the exact location where fission product precipitates were identified using the STEM, EELS and EDS techniques. Additionally, this will provide the opportunity to use other SEM facilities with higher resolution (higher speed) EBSD cameras to further enhance the quality of images obtained.

Acknowledgements

This work was sponsored by the U.S. Department of Energy, Office of Nuclear Energy, under DOE Idaho Operations Office Contract DE-AC07-05ID14517. James Madden is acknowledged for the FIB sample preparation. David Petti, James Cole and Paul Demkowicz are thanked for the review of this document.

References

- [1] H. Nabielek, P.E. Brown, P. Offerman, Nucl. Techn. 35 (1977) 483
- [2] P.A. Demkowicz, J.D. Hunn, R.N. Morris, J.M. Harp, P.L. Winston, C.A. Baldwin, F.C. Montgomery, "Preliminary Results of Post-Irradiation Examination of the AGR-1 TRISO Fuel Compacts," Paper HTR2012-3-021, Proceedings of the HTR 2012, Tokyo, Japan, October 28 – November 1, 2012.
- [3] D.P. Petti, TRISO-Coated Particle Fuel Phenomenon Identification and Ranking Tables (PIRTs) for Fission Product Transport Due to Manufacturing Operations, and Accidents, in, US, Nuclear Regulatory Commission, Washington, DC, 2004 (20555-0001).
- [4] IJ van Rooyen, ML Dunzik-Gougar, and PM van Rooyen, "Silver (Ag) Transport Mechanisms in TRISO Coated Particles," A Critical Review, Paper HTR2012-3-040, Proceedings of the HTR 2012, Tokyo, Japan, October 28 – November 1, 2012.
- [5] H. Nabielek, P. E. Brown, The Release of Silver -110m in High Temperature Reactors: Technical Note, OECD Dragon Project. Vol. 657, 1975 p. 370
- [6] T. J. Gerzcek, L. Tan, T. R. Allen, S. Khalil, D. Shrader, Y. Liu, D. Morgan, I. Szlufarska, Experimental and simulation insight on the transport of silver fission product in SiC", Paper HTR2008-58131, Proceedings of the HTR 2008, Washington DC, USA, September 28 – October 1, 2008.
- [7] E. Friedland, J. B. Malherbe, N. G. Van der Berg, H. Hlatshwayo, A, J. Botha, E. Wendler, W. Wesch, "Study of silver diffusion in silicon carbide", J Nucl Mater, 389 (2009) 326-331[8] E. Lopez-Honorato, D. X. Yang, J. Tan, P. J. Meadows, and P. Xiaow, "Silver Diffusion in Coated Fuel Particles," J. Am. Ceram. Soc., 93 [10] 3076-3079 (2010).
- [9] D. Schrader, S. M. Khalil, T. Gerzcek, T.R. Allen, A. J. Heim, I. Szlufarska, D. Morgan, "Ag diffusion in cubic silicon carbide", J Nucl Mater, 408 (2011) 257-271
- [10] S. Khalil, N. Swaminathan, D. Schrader, A. J. Heim, D.D. Morgan, I. Szlufarska, , "Diffusion of Ag along 3 grain boundaries in 3C-SiC", Physical Review B 84, 214104 (2011)
- [11] Y. Chen and A. Schuh, "Geometric Considerations for Diffusion in Polycrystalline Solids," J. Appl. Phys., 101, 063524, 12pp (2007).
- [12] H. J. Maclean, "Silver Transport in CVD Silicon Carbide", PhD Thesis, Department of Nuclear Engineering, MIT, Boston, 2004
- [13] IJ van Rooyen, DE Janney, BD Miller, PA Demkowicz, J. Riesterer, "Electron Microscopic Evaluation and Fission Product Identification of Irradiated TRISO Coated Particles from the AGR-1 Experiment," A Preliminary Review, Paper HTR2012-3-023, Proceedings of the HTR 2012, Tokyo, Japan, October 28 – November 1, 2012.
- [14] E.A. Brandes and G.B. Brook, eds., Smithells Metals Reference Book, Seventh Edition, 1992, Butterworth-Heinemann, Ltd.: Oxford
- [15] M. Barrachin, R. Dubourg, S. De Groot, M.P. Kissane, K. Bakker, Fission-product behaviour in irradiated TRISO-coated particles: Results of the HFR-EU1bis experiment and their interpretation . J Nucl Mater, 415 (2011) 104-116
- [16] K. Minato, T. Ogawa, K. Fakuda, H. Sekino, H. Miyaniishi, S. Kado, I. Takahasi, Release behaviour of metallic fission products from HTGR fuel particles at 1600 to 1900oC: J. Nucl. Mater. Vol. 202 (1993) 47 – 53
- [17] P. Demkowicz, K. Wright, J. Gan, D. Petti, High temperature interface reactions of TiC, TiN, and SiC with palladium and rhodium, Solid State Ionics, Volume 179, Issue 39, 15 December 2008, 2313–2321
- [18] J. Neethling, J. O'Connell, J. Olivier, Palladium assisted silver transport in polycrystalline SiC, AG-PD HTR2010-196
- [19] J. Maki. AGR-1 Irradiation Experiment Test Plan INL/EXT-05-00593 rev 3 10/20/09
- [20] D.B. Williams and C.B. Carter, "Transmission Electron Microscopy," A Textbook for Materials Science, Plenum Press, New York, 1996.
- [21] Gatan: A Chart of Inner Shell Loss Edge Types and Energies for Electron Energy Loss Spectroscopy.